

RESEARCH ARTICLE

Nuclear envelope-distributed *CD147* interacts with and inhibits the transcriptional function of *RING1* and promotes melanoma cell motility

Junchen Chen^{1,2}, Cong Peng^{1,2}, Li Lei^{1,2}, Jianglin Zhang^{1,2}, Weiqi Zeng^{1,2*}, Xiang Chen^{1,2*}

1 Department of Dermatology, Xiangya Hospital, Central South University, Changsha, Hunan, P.R. China, **2** Hunan Key Laboratory of Skin Cancer and psoriasis, Central South University, Changsha, Hunan, P.R. China

* Weiqizeng@gmail.com(WQZ); chenxiangck@126.com(XC)



OPEN ACCESS

Citation: Chen J, Peng C, Lei L, Zhang J, Zeng W, Chen X (2017) Nuclear envelope-distributed *CD147* interacts with and inhibits the transcriptional function of *RING1* and promotes melanoma cell motility. PLoS ONE 12(8): e0183689. <https://doi.org/10.1371/journal.pone.0183689>

Editor: Salvatore V. Pizzo, Duke University School of Medicine, UNITED STATES

Received: May 16, 2017

Accepted: August 9, 2017

Published: August 23, 2017

Copyright: © 2017 Chen et al. This is an open access article distributed under the terms of the [Creative Commons Attribution License](https://creativecommons.org/licenses/by/4.0/), which permits unrestricted use, distribution, and reproduction in any medium, provided the original author and source are credited.

Data Availability Statement: All relevant data are within the paper and its Supporting Information files.

Funding: This work was supported by grant 81430075 from the National Natural Science Foundation of China (Xiang Chen), grant 81620108024 from International Cooperation and Exchanges National Natural Science Foundation of China (Xiang Chen), and grant 81572677 from the National Natural Science Foundation of China (Weiqi Zeng). <http://www.nsf.gov.cn>.

Abstract

Melanoma accounts for nearly 80% of all deaths associated with skin cancer. *CD147* plays a very important role in melanoma progression and the expression level may correlate with tumor malignancy. *RING1* can bind DNA and act as a transcriptional repressor, play an important role in the aggressive phenotype in melanoma. The interactions between *CD147* and *RING1* were identified with a yeast two-hybrid and *RING1* interacted with *CD147* through the transmembrane domain. *RING1* inhibits *CD147*'s capability promoting melanoma cell migration. In conclusion, the study identified novel interactions between *CD147* and *RING1*, recovered *CD147* nuclear envelope distribution in melanoma cells, and suggested a new mechanism underlying how cytoplasmic *CD147* promotes melanoma development.

Introduction

Although melanoma represents only 4% of all skin cancers, it accounts for nearly 80% of all deaths associated with skin cancer [1–3]. Accumulating data show that melanoma progression involves a series of genetic and environmental changes, including enhanced anaerobic glycolysis, microenvironment remodeling caused by matrix metalloproteinase (MMPs), genome epigenetic modification changes and angiogenesis.

CD147, a type I integral membrane receptor protein that belongs to the immunoglobulin superfamily [4], is a widely expressed integral plasma membrane glycoprotein that stimulates the secretion of extracellular MMPs, also known as a membrane extracellular matrix metalloproteinase inducer (*EMMPRIN/Basigin*) [5–7]. It consists of two Ig-like extracellular domains, a transmembrane domain and a cytoplasmic domain. Its transmembrane domain contains highly conserved glutamic acid residues and leucine zipper-like sequences, allowing it to interact with multiple signaling proteins of other membrane proteins [8]. The expression level of *CD147* in many tumor cells may correlate with tumor malignancy [9–11].

Competing interests: The authors have declared that no competing interests exist.

CD147 is primarily distributed on the cellular membrane in multiple types of human tissues, and it has been shown to regulate the function of many membrane proteins, such as *MCTs* [12, 13], *GLUTs* [14], *ABCGs* [15, 16] and *Integrins* [17]. To date, most investigations on *CD147* have focused on its cellular membrane functions [18, 19]. Interestingly, we have found that in metastatic malignant melanomas, *CD147* is largely redistributed in cellular inner membrane systems [20], such as the mitochondrial membrane [21], ER [22] and nuclear envelope. *CD147* interacts with Ubiquinone Oxidoreductase Subunit S6 (*NDUFS6*) on the mitochondrial membrane and regulates the oxidative phosphorylation process and is required for melanoma cell glucose metabolism. It also interacts with Calcium Modulating Ligand (*CAMLG*) in the endoplasmic reticulum (ER) and regulates calcium homeostasis in melanoma cells.

PcG proteins also play an important role in the aggressive phenotype in melanoma [23]. The PcG proteins form two distinct complexes: EED-EZH2 and the PRC complex [24]. *RING1* is part of the *PRC1* complex and contributes to PcG protein function. *RING1* proteins belong to the *RING* finger family of proteins characterized by a *RING* domain, which is a zinc-binding motif related to the zinc finger domain. *RING1* can bind DNA and act as a transcriptional repressor [25].

The matrix Gla protein (MGP) is initially isolated from the bone tissue and is also expressed in kidney, lung, heart, cartilage and vascular smooth muscle cells. [26]. It is up-regulated in a variety of tumors, including ovarian, breast, urogenital and skin tumors [27–31].

Our preliminary data from a yeast two-hybrid system have shown that several nuclear proteins interact with *CD147* in vitro, including *RING1*. In this study, we investigated the details of the interactions and functions of nuclear protein *RING1* in the regulation of downstream gene transcription.

Materials and methods

Cell culture

The human malignant melanoma cell line A375 was obtained from the American Type Culture Collection. The A375 cells expressing recombinant plasmid SUPER/CD147 short hairpin RNA (shRNA) (A375 ShCD147) or recombinant plasmid SUPER/RING1 short hairpin RNA (shRNA) (A375 ShRING1) or empty vector (A375 EV). These cells were maintained in RPMI 1640 medium (Thermo Scientific, MA, USA) supplemented with 10% FBS (Thermo Scientific, MA, USA). The 293T cell line was purchased from Clontech (Clontech, CA, USA) and grown in Dulbecco's modified Eagle's medium (DMEM) supplemented with 10% FBS. All cell lines were maintained in a humidified 5% CO₂ atmosphere at 37°C.

PCR and cloning

Wild type *CD147* and deletion mutants were fused to a transcript encoding Myc, and wild type *RING1* was fused to a transcript encoding Flag. Deletion mutants of *CD147* and the full length (FL) *RING1* promoter were amplified by PCR. The pcDNA4ToA and pcDNA3ToA plasmids (Promega, WI, USA) were double digested with the same restriction enzymes. Both PCR products and plasmids were recovered from 1.5% agarose gels and ligated using T4 ligase (Takara Bio, Otsu, Japan) to yield pcDNA4ToA-CD147 and pcDNA3ToA-RING1. After a 1 h of incubation at room temperature, plasmids of colonies grown on ampicillin-containing LB medium. Positive colonies were identified by PCR and direct sequencing. PCR was performed using the primers listed in S1 Table.

RNA analysis

Total RNA was isolated from cells with TRIzol (Invitrogen, CA, USA) according to the manufacturer's instructions. RNA was dissolved in 60 μ l of DEPC-treated water. Reverse transcription and real-time PCR (RT-PCR) were performed with 2 μ g of total RNA using Reverse Transcriptase AMV (Takara Bio, Otsu, Japan) and Premix Ex Taq™ II kit (Takara Bio, Otsu, Japan) according to the manufacturer's instructions. The primers are listed in [S1 Table](#).

The yeast two-hybrid screen

A human fetal cDNA library and a yeast two-hybrid(Y2H) system were purchased from Clontech (Cat. 637242). Wild type *CD147* was reverse transcribed and the cDNA amplified and inserted into pGBKT7 to yield pGBKT7-*CD147*. This recombinant plasmid and the library plasmids containing the human fetal brain cDNA library were co-transformed into the AH109 yeast strain. After screening according to the manufacturer's instructions, the prey plasmids were purified from positive clones and yeast co-transformed with pGBKT7-*CD147* and prey plasmid to verify the interaction. These transformants with both bait and prey plasmids were plated on synthetic defined dropout medium. Transformants with non-interacting protein pairs were able to grow on media lacking leucine and tryptophan (SD/-Leu/-Trp or -2 SD medium), while only positive clones containing interacting prey and bait proteins were able to grow on dropout medium lacking tryptophan, leucine, histidine, and adenine (SD/-Leu/-Trp/-His/-Ade or -4 SD medium). The positive colonies were lysed and subjected to the ortho-nitrophenyl-b-D-galactopyranoside (ONPG) assay to verify the interaction. Finally, confirmed positive colonies were picked and individual plasmids amplified, purified, and analyzed by sequencing.

Immunoprecipitation and Western blotting

Briefly, according to the TurboFect Transfection manual (Thermo Scientific). When 293T cells grew to 70–80% were co-transfected with plasmids for 36 h. After the cells were lysed and were centrifuged at 12,000 rpm for 15 min and the supernatant protein concentration was determined by a BCA protein assay (Santa Cruz, CA, USA) for co-immunoprecipitation (CO-IP). Proteins were incubated with magnetic beads linked to anti-Flag (Sigma), anti-Myc (Santa Cruz), anti-CD147 (Abcam, Cambridge, UK), or control IgG and then with protein A/G beads (Sigma) for overnight 4°C. All of the beads were washed with phosphate-buffered saline (PBS), added to 40 μ l lysis buffer plus 10 μ l of loading buffer and incubated at 95°C for 5 min. The proteins were separated by SDS-PAGE and electroblotted onto to polyvinylidene difluoride (PVDF) membranes (Millipore, MA, USA). The immunoblots were probed with anti-Myc (Santa Cruz, 1:1000), anti-Flag (Sigma, 1:10,000), anti-CD147 (Abcam, 1:1000), anti-RING1 (Abcam, 1:100), or anti- β -actin (Sigma, 1:10,000) overnight at 4°C being blocked in medium containing 5% non-fat milk, TBS (25 mM Tris balanced to pH 8.0, 150 mM NaCl) and 0.1% Tween 20. Immunolabeled proteins were then treated with goat anti-mouse antibody (Sigma, 1:10,000) for 1 hour at room temperature and subsequently treated with goat anti-mouse IgG-HRP antibody or a goat anti-rabbit antibody (Sigma, 1:10,000). The immunoblots were developed with an enhanced chemiluminescence detection system (Bio-Rad, CA, USA).

Immunofluorescence staining

The transfected A375 cells or the A375 cells without transfection were grown on glass coverslips. After washing with PBS, both the transfected A375 cells or the A375 cells without transfection were fixed, permeabilized and were incubated with 1% BSA in PBS (adjusted pH value

to 7.2–7.4) for 1 h at room temperature. The cells were then incubated with with mouse anti-Myc (Santa Cruz, 1:100) and rabbit anti-Flag (Sigma, 1:100) or mouse anti-CD147 (Abcam, 1:100) and rabbit anti-RING1 (Santa Cruz, 1:50) in a humidified box for 4°C overnight. Immunolabeling was visualized by incubation in Alexa Fluor-conjugated secondary antibodies (Invitrogen, 1:200) for 1 h at room temperature. The slides were covered with Vectashield Mounting medium containing DAPI (Vector Laboratories, CA, USA) and viewed under an inverted fluorescence microscope (Leica, Solms, Germany).

Design and transfection of siRNA targeting *CD147* and *RING1*

The small interfering RNAs (siRNAs) were designed using siDirect2.0 software (<http://sidirect2.rnai.jp/>) and synthesized by GenePharma Company (Shanghai, China). Two siRNAs targeting *CD147* mRNA, si-1039 and si-1207, and one siRNA targeting *RING1* mRNA (si-1039 sense 5′-ACAUAAAAGCACAAAAAUGGC-3′ and anti-sense 5′-CAUUUUUGUGCUUUUAUGUUU-3′, si-1207 sense 5′-CAUACACUCCUUCUUUUUA-3′ and anti-sense 5′-AAAAAG AAGGAAGUGUAUGAU-3′). A scrambled siRNA (GenePharma) that does not target any gene was used as a negative control siRNA. A375 cells were transfected with siRNA and transfection reagent according to the manufacturer's instructions. Briefly, A375 cells were seeded in 35mm dishes at a density of 2×10^5 cells/well with 2 ml of RPMI 1640 and transfected with 75 pmol si-1039 or si-1207 using 7.5 μl/dish of Lipofectamine RNAiMAX (Invitrogen) according to the manufacturer's instructions. After 72 h, cells were collected for RNA and protein to determine the efficiency of *CD147* knockdown by western blotting or RNA Analysis.

Results

Identification of *CD147* that interacts with *RING1*

To identify the cellular targets or possible interactive molecules with *CD147*, we used Y2H screening. The yeast strain AH109 was transformed with two proteins (namely bait and prey) are fused to the activation domain (AD) or the DNA-binding domain (BD) of the Gal 4 transcription factor and, if interaction occurs, Gal4 activates a set of reporter genes. The open reading frame (ORF) of *CD147* was cloned in frame with the GAL4 DNA-BD of pGBKT7. If the *CD147* could interact with some proteins it allows yeast to grow in dropout media. Among the positive clones, we focused on *RING1* as a possible binding partner with *CD147*. To identify the result, the yeast strain AH109 was transformed with *CD147* and either EV or *RING1* and plated on dropout medium. Fig 1A shows that only the presence of *CD147* and *RING1* allowed for growth of the transformants on -4SD medium. To confirm the interaction, the positive colonies were subjected to an ONPG assay (Fig 1A). To verify the results of the Y2H screen, we performed immunofluorescence staining and CO-IP. 293T cells expressing exogenous *CD147* and *RING1* stained with PE-conjugated anti-RING1 (red) and FITC-conjugated anti-*CD147* (green) display partial co-localization in the emphasized regions surrounding the nuclear envelope (Fig 1B). After the 293 T cells were transfected with *CD147*-MYC and Flag-*RING1* plasmids, the cell lysates were resolved by 10% SDS-PAGE and probed for the presence of *CD147* or *RING1* using anti-*CD147* protein mAb, as evidenced by CO-IP, thereby indicating a *CD147*-*RING1* interaction (Fig 1C). These results confirmed that *CD147* was able to interact with *RING1*.

CD147 colocalizes with *RING1* dependent on transmembrane domain

We previously indicated that *CD147* was able to interact with *RING1*. To further investigate the influence factors of the colocalization, we constructed the mutants of *CD147*. The full-

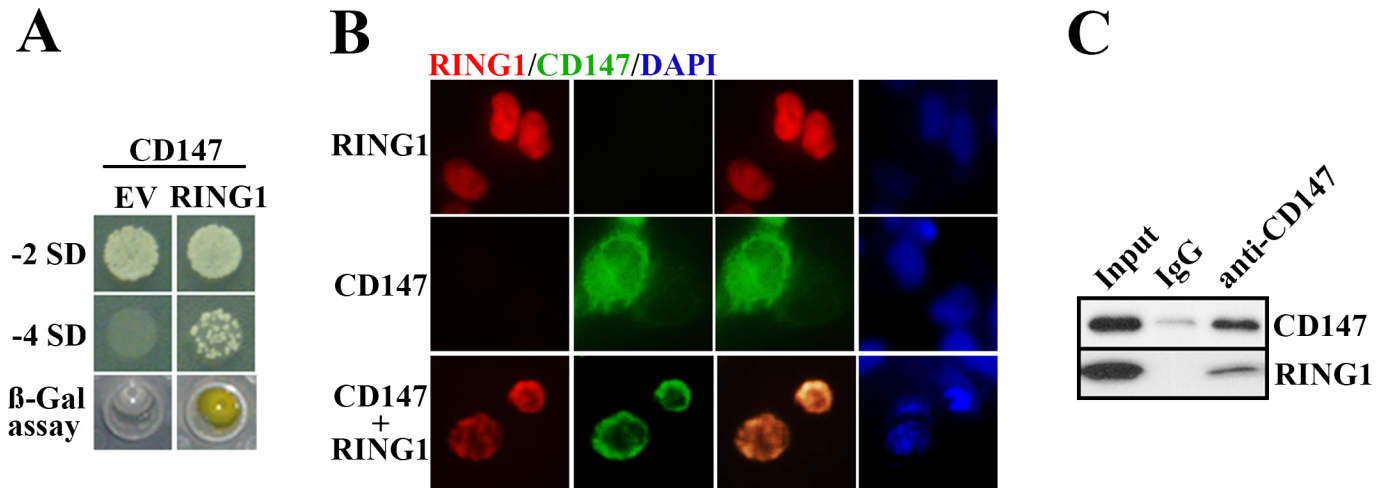


Fig 1. The interaction between RING1 and CD147 in vitro. RING1 colocalizes with CD147 proteins on the nuclear envelope of melanoma cells. (A) Clones were abundant in both -2 SD and -4 SD culture media when the yeast cells were transfected with RING1 and CD147 compared with yeast cells transfected with CD147 and EV. In these colonies, the ONPG-containing medium became a yellow color, thus confirming the interaction between RING1 and CD147. By comparison, the yeast co-transfected with CD147 and EV produced no viable colonies, and the ONPG assay was negative. (B) Exogenous CD147 and RING1 were co-localized in regions surrounding the nuclear envelope in 293T cells, as identified by immunofluorescence staining. (C) 293T cells were harvested and subjected to immunoprecipitation (IP) with mouse normal IgG and anti-CD147 Ab. The membranes were further probed with the indicated antibodies.

<https://doi.org/10.1371/journal.pone.0183689.g001>

length protein is composed of two extracellular immunoglobulin (Ig) domains with a total of 185 amino acids (aa), 39 aa cytoplasmic domains and 24 aa transmembrane domains (Fig 2A). Each domain can interact with different proteins. We synthesized five different CD147 deletion mutants and then the plasmids as the indicated images shown were co-transfected into the eukaryotic expression plasmid pcDNA4ToA, which adds the Myc epitope to the C-terminus of the inserted gene. The expression was detected by western blotting (Fig 2C). By Immunofluorescence staining observations it was found that the co-localization of the proteins is evident in all cells, as shown by the yellow region on the combined image, except in those expressing the deletion mutant D207-269 (lacking transmembrane and intracellular domains), so as to devas-tate that the transmembrane region is essential for RING1 and CD147 interaction (Fig 2B).

CD147 gene knockdown in A375 cells affected downstream gene expressions

Through siRNA interference technology, we knocked down the CD147 gene in A375 cells, and used gene chip technology to investigate the effect of CD147 on downstream gene transcrip-tome. By examining the heatmap (Fig 3A), we found that after knockdown of CD147, tran-scriptome analysis showed at least 67 up-regulated genes and 115 down-regulated genes(S2 Table). To further validate the results, RT-PCR was performed, and the results were consistent with the transcription group sequencing (Fig 3B).

Reduced RING1 expression reverses the decrease in MGP expression caused by CD147 depletion

In A375 cells (SiCD147-A375), CD147 knockdown resulted in a decrease in MGP mRNA expres-sion (Fig 4A), whereas knockdown of RING1 in SiCD147-A375 cells rescued the expression of MGP mRNA. Furthermore, to verify the change in mRNA, RING1 knockdown in siCD147-A375 was confirmed by western blot analysis to restore the expression of MGP (Fig 4B).

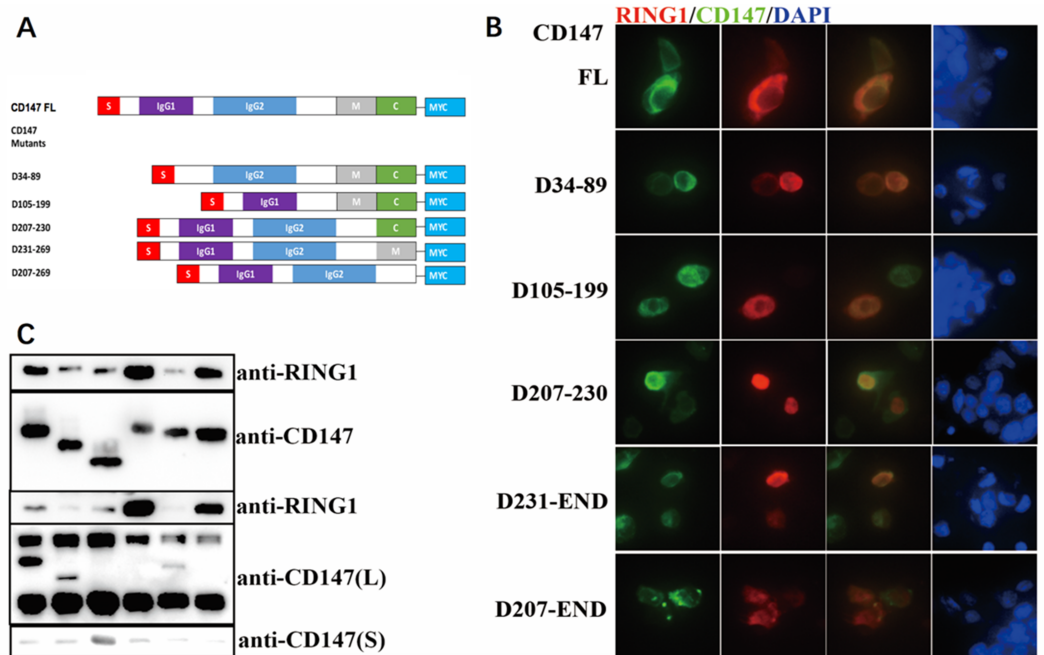


Fig 2. CD147 colocalizes with RING1 dependent on transmembrane domain. (A) An illustration of the CD147 mutants (left) used in CO-IP and immunofluorescence experiments; 34–87: 1st IgG (IgG1); 105–199: 2nd IgG (IgG2); 207–230: transmembrane (M); 231–269: cytoplasmic domain (C). (B) The A375 cells co-transfected with Flag-RING1 and different CD147-MYC deletion mutants were stained with fluorophore-conjugated anti-Flag (red) and anti-Myc (green). The CD147 mutants without the transmembrane domain (D207-230 and D207-269) showed no co-localization with RING1. (C) Cells (293T) were co-transfected with plasmids encoding Flag-RING1 and different CD147-MYC deletion mutants. Transfected 293T cells were subjected to IP with anti-Flag Ab. The immunoprecipitates and the whole cell lysates were further analyzed by IB with anti-Flag Ab and anti-Myc Ab.

<https://doi.org/10.1371/journal.pone.0183689.g002>

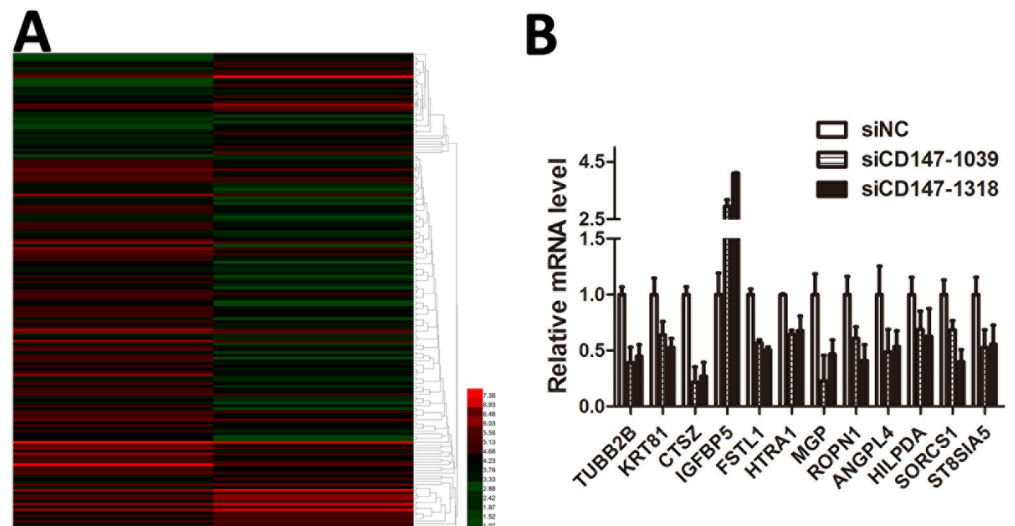


Fig 3. CD147 gene knockdown in A375 cells affected many gene translation pathways, thus leading to the differential expression of hundreds of genes. (A) Heatmap representing the expression levels of genes; red (normal) and green (siCD147) colors indicate the up- and down-regulated genes. Transcriptome analysis demonstrated 67 up-regulated and 115 down-regulated genes in A375 cells transfected with siCD147. (B) Several genes referred to in A were shown to be up- or down-regulated in A375 cells by RT-PCR. The result was consistent with the transcriptome analysis.

<https://doi.org/10.1371/journal.pone.0183689.g003>

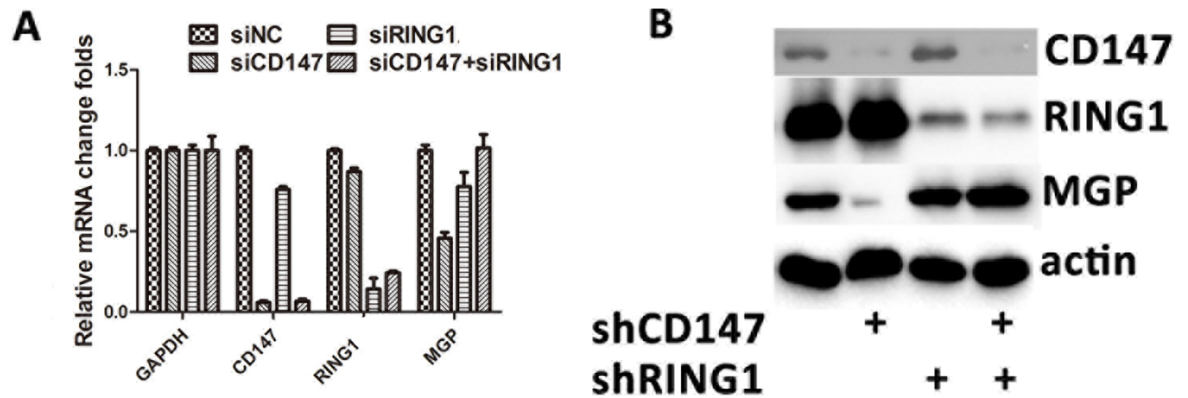


Fig 4. Reduction of MGP caused by CD147 depletion was rescued by RING1 depletion. (A) CD147 knockdown in A375 cells (SiCD147-A375) led to the decreased expression of MGP mRNA. Knockdown of RING1 in siCD147-A375 cells rescued the expression of MGP mRNA. (B) RING1 knockdown in siCD147-A375 cells rescued the expression of MGP, as shown by western blotting analysis.

<https://doi.org/10.1371/journal.pone.0183689.g004>

RING1 inhibits CD147's capability promoting melanoma cell migration

Cell migration was assessed with a wound healing assay, and in the A375 cells transfected with shCD147 and A375 cells transfected with shCD147 and shRING1. The effect of depletion of CD147 is significant in invasive capacities of both of the co-transduced tumors cell by comparing shGFP-shGFP (upper lane, third picture) and shGFP-shCD147 (upper lane, fourth picture) (Fig 5A). With CD147, cells completely rescued the gap at 48 hrs, while only 44% gap can be rescued under CD147 depletion condition. Comparing to shGFP-shCD147, shRING1-shCD147 show 79% and 66% rescued gaps at two different shRNA targets (Fig 5B). That suggests depletion RING1 under CD147 knockdown background can rescue the cell motility.

Discussion

CD147 has been found to be related to cancer development because of its ability to regulate multiple different pathways, including up-regulating MMPs levels, recruiting MCTs to

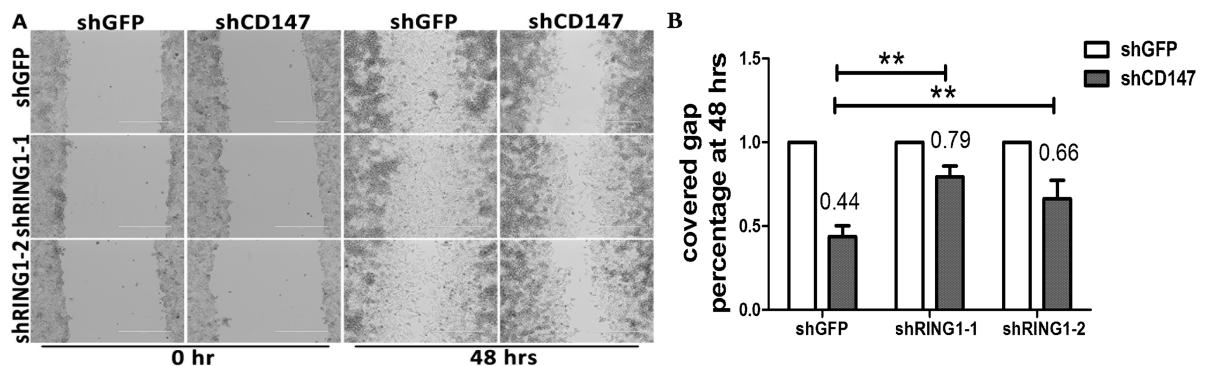


Fig 5. RING1 depletion led to impaired migration ability in A375 cells transfected with shCD147. (A) Cell migration was assessed with a wound healing assay by measuring the distance between the wound edges at the indicated time points in both A375 cells transfected with shCD147 and A375 cells transfected with shCD147 and shRING1. (B) Five random experiments were performed. The gap was measured by Image plus 6.0 software. The ratio of the gap at 48 h to 0 h was analyzed using GraphPad software; t-tests were performed, and the p values are represented by a double asterisk (**, p<0.01).

<https://doi.org/10.1371/journal.pone.0183689.g005>

membrane localizations, and enhancing glycolysis by promoting expression of GLUTs [32–34]. Almost all of the functions of CD147 that have been investigated to date have been associated with the membrane portion of CD147[35]. We have previously reported that CD147 distributes to the cytoplasm in certain metastatic melanomas and have identified novel functions of CD147 in the endoplasmic reticulum (ER), including maintaining both calcium homeostasis and mitochondrial function [21, 36]. This study identified the nuclear envelope distribution of CD147 in melanoma and highlights a novel mechanism of CD147 in controlling melanoma metastasis.

A nuclear envelope protein that regulates transcription has been identified. Lamin is a typical nuclear protein with a role in maintaining nuclear structure. A recent investigation has shown that lamin on the nuclear envelope recruits certain transcriptional factors and inhibits their transcriptional activities by sequestering them at the nuclear envelope and may preventing them from interacting with DNA[37]. We found that CD147 plays a similar role on the nuclear envelope. RING1 expression in cells with CD147 knockdown showed a clear distribution throughout the nucleus but RING1 recruitment was observed after co-expression with CD147. CD147 is a 'binding protein' that regulates many membrane functional proteins by recruiting them to the membrane. On the basis of our previous results, CD147 binds many partners through its transmembrane domain[19]. This finding suggests that the binding may be a lyophobic association, which is less specific than a protein-protein interaction based on domain structure. Thus, RING1 may not be the only target of CD147 on the nuclear envelope. In future work, we are planning to use a biotin-based method to identify the potential targets.

Epigenetic modification changes have been connected with cancer development [38]. RING1 can modify histone ubiquitination in the promoter regions of certain downstream target genes [39]. In our RNA-seq data, the numbers of genes expressed changed when CD147 was depleted by siRNA, but the expression of only MGP and ANGPTL4 (ANGPTL4 data not shown) genes was rescued when RING1 was co-depleted. We presume that this difference might have been caused by insufficient sensitivity of the RNA-seq. Many downstream target genes have been identified and will be verified individually through real-time PCR in our future studies.

Conclusions

In conclusion, our study identified novel interactions between CD147 and RING1, recovered CD147 nuclear envelope distribution in melanoma cells, and suggested a new mechanism underlying how cytoplasmic CD147 promotes melanoma development.

Supporting information

S1 Table. The primers of RNA analysis.
(DOCX)

S2 Table. The mRNAs of CD147 gene knockdown or not in A375 cells by microarray meta-analysis.
(XLSX)

Author Contributions

Investigation: Weiqi Zeng.

Methodology: Cong Peng, Li Lei, Xiang Chen.

Project administration: Cong Peng, Xiang Chen.

Resources: Jianglin Zhang, Weiqi Zeng, Xiang Chen.

Writing – original draft: Junchen Chen, Weiqi Zeng.

Writing – review & editing: Junchen Chen, Weiqi Zeng, Xiang Chen.

References

1. Korn EL, Liu PY, Lee SJ, Chapman JAW, Niedzwiecki D, Suman VJ, et al. Meta-analysis of phase II cooperative group trials in metastatic stage IV melanoma to determine progression-free and overall survival benchmarks for future phase II trials. *Journal of Clinical Oncology*. 2008; 26(4):527–34. <https://doi.org/10.1200/JCO.2007.12.7837> PMID: 18235113
2. Siegel R, Ward E, Brawley O, Jemal A. Cancer statistics, 2011. *Ca A Cancer Journal for Clinicians*. 2010; 60(5):277–300. <https://doi.org/10.3322/caac.20073> PMID: 20610543
3. Ferlay J, Steliarova-Foucher E, Lortet-Tieulent J, Rosso S, Coebergh JWW, Comber H, et al. Reprint of: Cancer incidence and mortality patterns in Europe: Estimates for 40 countries in 2012 ☆. *European Journal of Cancer*. 2015; 51(9):1201–2.
4. Biswas C, Zhang Y, Decastro R, Guo H, Nakamura T, Kataoka H, et al. The human tumor cell-derived collagenase stimulatory factor (renamed EMMPRIN) is a member of the immunoglobulin superfamily. *Cancer Research*. 1995; 55(2):434–9. PMID: 7812975
5. Schneider T, Reiter C, Eule E, Bader B, Lichte B, Nie Z, et al. Characterization of basigin isoforms and the inhibitory function of basigin-3 in human hepatocellular carcinoma proliferation and invasion. *Molecular & Cellular Biology*. 2011; 31(13):2591–604.
6. Sweeny L, Liu Z, Bush BD, Hartman Y, Zhou T, Rosenthal EL. CD147 and AGR2 expression promote cellular proliferation and metastasis of head and neck squamous cell carcinoma. *Experimental Cell Research*. 2012; 318(14):1788–98. <https://doi.org/10.1016/j.yexcr.2012.04.022> PMID: 22659167
7. Lescaille G, Menashi S, Cavelier-Balloy B, Khayati F, Quemener C, Podgorniak MP, et al. EMMPRIN/CD147 up-regulates urokinase-type plasminogen activator: implications in oral tumor progression. *Bmc Cancer*. 2012; 12(1):115.
8. Nabeshima K, Iwasaki H, Koga K, Hojo H, Suzumiya J, Kikuchi M. Emmprin (basigin/CD147): matrix metalloproteinase modulator and multifunctional cell recognition molecule that plays a critical role in cancer progression. *Pathology international*. 2006; 56(7):359–67. Epub 2006/06/24. <https://doi.org/10.1111/j.1440-1827.2006.01972.x> PMID: 16792544.
9. Piao S, Zhao S. Increased expression of CD147 and MMP-9 is correlated with poor prognosis of salivary duct carcinoma. *Journal of Cancer Research & Clinical Oncology*. 2012; 138(4):627–35.
10. Bi XC, Liu JM, Zheng XG, Xian ZY, Feng ZW, Lou YX, et al. Over-expression of extracellular matrix metalloproteinase inducer in prostate cancer is associated with high risk of prostate-specific antigen relapse after radical prostatectomy. *Clinical & Investigative Medicine Medecine Clinique Et Experimentale*. 2011; 34(6):E358–E.
11. Gabison EE, Huet E, Baudouin C, Menashi S. Direct epithelial-stromal interaction in corneal wound healing: Role of EMMPRIN/CD147 in MMPs induction and beyond. *Progress in Retinal & Eye Research*. 2009; 28(1):19–33.
12. Walters DK, Arendt BK, Jelinek DF. CD147 regulates the expression of MCT1 and lactate export in multiple myeloma cells. *Cell Cycle*. 2013; 12(19):3175–83. <https://doi.org/10.4161/cc.26193> PMID: 24013424
13. Xia K, Chen Y, Pei W, Xing J, Chen Z. Upregulation of CD147 protects hepatocellular carcinoma cell from apoptosis through glycolytic switch via HIF-1 and MCT-4 under hypoxia. *Hepatology International*. 2014; 8(3):405–14. <https://doi.org/10.1007/s12072-014-9536-6> PMID: 26202642
14. Huang XQ, Chen X, Xie XX, Zhou Q, Li K, Li S, et al. Co-expression of CD147 and GLUT-1 indicates radiation resistance and poor prognosis in cervical squamous cell carcinoma. *International Journal of Clinical & Experimental Pathology*. 2014; 7(4):1651–66.
15. Zhou S, Liao L, Chen C, Zeng W, Liu S, Su J, et al. CD147 mediates chemoresistance in breast cancer via ABCG2 by affecting its cellular localization and dimerization. *Cancer Letters*. 2013; 337(2):285–92. <https://doi.org/10.1016/j.canlet.2013.04.025> PMID: 23623923
16. Zhao S, Chen C, Liu S, Zeng W, Su J, Wu L, et al. CD147 promotes MTX resistance by immune cells through up-regulating ABCG2 expression and function. *Journal of Dermatological Science*. 2013; 70(3):182–9. <https://doi.org/10.1016/j.jdermsci.2013.02.005> PMID: 23622764
17. Wu J, Li Y, Dang YZ, Gao HX, Jiang JL, Chen ZN. HAb18G/CD147 promotes radioresistance in hepatocellular carcinoma cells: a potential role for integrin $\beta 1$ signaling. *Molecular Cancer Therapeutics*. 2015; 14(2):553–63. <https://doi.org/10.1158/1535-7163.MCT-14-0618> PMID: 25534361

18. Knutti N, Kuepper M, Friedrich K. Soluble extracellular matrix metalloproteinase inducer (EMMPRIN, EMN) regulates cancer-related cellular functions by homotypic interactions with surface CD147. *Febs Journal*. 2015; 282(21).
19. Takashi M. Basigin (CD147), a multifunctional transmembrane glycoprotein with various binding partners. *Journal of Biochemistry*. 2015; 159(5):481–90. <https://doi.org/10.1093/jb/mvv127> PMID: [26684586](https://pubmed.ncbi.nlm.nih.gov/26684586/)
20. Zeng W, Su J, Wu L, Yang D, Long T, Li D, et al. CD147 promotes melanoma progression through hypoxia-induced MMP2 activation. *Current Molecular Medicine*. 2014; 14(1):163–73. PMID: [24090196](https://pubmed.ncbi.nlm.nih.gov/24090196/)
21. Luo Z, Zeng W, Tang W, Long T, Zhang J, Xie X, et al. CD147 Interacts with NDUFS6 in Regulating Mitochondrial Complex I Activity and the Mitochondrial Apoptotic Pathway in Human Malignant Melanoma Cells. *Current Molecular Medicine*. 2014; 14(10):1252–64. PMID: [25470292](https://pubmed.ncbi.nlm.nih.gov/25470292/)
22. Long T, Su J, Tang W, Luo Z, Liu S, Liu Z, et al. A novel interaction between calcium-modulating cyclophilin ligand and Basigin regulates calcium signaling and matrix metalloproteinase activities in human melanoma cells. *Cancer Letters*. 2013; 339(1):93–101. <https://doi.org/10.1016/j.canlet.2013.07.019> PMID: [23879967](https://pubmed.ncbi.nlm.nih.gov/23879967/)
23. Mchugh JB, Fullen DR, Ma L, Kleer CG, Su LD. Expression of polycomb group protein EZH2 in nevi and melanoma. *Journal of Cutaneous Pathology*. 2007; 34(8):597–600. <https://doi.org/10.1111/j.1600-0560.2006.00678.x> PMID: [17640228](https://pubmed.ncbi.nlm.nih.gov/17640228/)
24. Ru C, Tsukada YI, Yi Z. Role of Bmi-1 and Ring1A in H2A Ubiquitylation and Hox Gene Silencing. *Molecular Cell*. 2005; 20(6):845–54. <https://doi.org/10.1016/j.molcel.2005.12.002> PMID: [16359901](https://pubmed.ncbi.nlm.nih.gov/16359901/)
25. Endoh M, Endo T, Endoh T, Fujimura Y, Ohara O, Toyoda T, et al. Polycomb group proteins Ring1A/B are functionally linked to the core transcriptional regulatory circuitry to maintain ES cell identity. *Development*. 2008; 135(8):1513–24. <https://doi.org/10.1242/dev.014340> PMID: [18339675](https://pubmed.ncbi.nlm.nih.gov/18339675/)
26. Cancela L, Hsieh CL, Francke U, Price PA. Molecular structure, chromosome assignment, and promoter organization of the human matrix Gla protein gene. *Journal of Biological Chemistry*. 1990; 265(25):15040–8. PMID: [2394711](https://pubmed.ncbi.nlm.nih.gov/2394711/)
27. Chen L, O'Bryan JP, Smith HS, Liu E. Overexpression of matrix Gla protein mRNA in malignant human breast cells: isolation by differential cDNA hybridization. *Oncogene*. 1990; 5(9):1391–5. PMID: [2216462](https://pubmed.ncbi.nlm.nih.gov/2216462/)
28. Chen Y, Miller C, Mosher R, Zhao X, Deeds J, Morrissey M, et al. Identification of cervical cancer markers by cDNA and tissue microarrays. *Cancer Research*. 2003; 63(8):1927–35. PMID: [12702585](https://pubmed.ncbi.nlm.nih.gov/12702585/)
29. Hough CD, Cho KR, Zonderman AB, Schwartz DR, Morin PJ. Coordinately up-regulated genes in ovarian cancer. *Cancer Research*. 2001; 61(10):3869–76. PMID: [11358798](https://pubmed.ncbi.nlm.nih.gov/11358798/)
30. Levedakou EN, Strohmeier TG, Effert PJ, Liu ET. Expression of the matrix Gla protein in urogenital malignancies. *International Journal of Cancer*. 1992; 52(4):534–7. PMID: [1399132](https://pubmed.ncbi.nlm.nih.gov/1399132/)
31. P M, K K, M O, C S, S S, P L, et al. In situ identification of genes regulated specifically in fibroblasts of human basal cell carcinoma. *Journal of Investigative Dermatology*. 2007; 127(6):1516–23. <https://doi.org/10.1038/sj.jid.5700714> PMID: [17273163](https://pubmed.ncbi.nlm.nih.gov/17273163/)
32. Agrawal SM, Yong VW. The many faces of EMMPRIN—Roles in neuroinflammation. *Biochimica Et Biophysica Acta*. 2011; 1812(2):213–9. <https://doi.org/10.1016/j.bbadis.2010.07.018> PMID: [20674741](https://pubmed.ncbi.nlm.nih.gov/20674741/)
33. Weidle UH, Scheuer W, Eggle D, Klostermann S, Stockinger H. Cancer-related issues of CD147. *Cancer Genomics & Proteomics*. 2010; 7(3):157–69.
34. Su J, Gao T, Jiang M, Wu L, Zeng W, Zhao S, et al. CD147 silencing inhibits tumor growth by suppressing glucose transport in melanoma. *Oncotarget*. 2015.
35. Grass GD, Lu D, Qin Z, Parsons C, Toole BP. Chapter Thirteen – CD147: Regulator of Hyaluronan Signaling in Invasiveness and Chemoresistance. *Advances in Cancer Research*. 2014; 123:351–73. <https://doi.org/10.1016/B978-0-12-800092-2.00013-7> PMID: [25081536](https://pubmed.ncbi.nlm.nih.gov/25081536/)
36. Bartels H, Spring P. Determination of Isonicotinic Acid Hydrazide in Serum. *Chemotherapy*. 1975; 21(1):1–10. PMID: [238799](https://pubmed.ncbi.nlm.nih.gov/238799/)
37. Burke B, Stewart CL. The nuclear lamins: flexibility in function. *Nature Reviews Molecular Cell Biology*. 2012; 14(1):13–24. <https://doi.org/10.1038/nrm3488> PMID: [23212477](https://pubmed.ncbi.nlm.nih.gov/23212477/)
38. Piunti A, Shilatifard A. Epigenetic balance of gene expression by Polycomb and COMPASS families. *Science*. 2016; 352(6290).
39. Zhou W, Wei W, Sun Y. Genetically engineered mouse models for functional studies of SKP1-CUL1-F-box-protein (SCF) E3 ubiquitin ligases. *Cell Research*. 2013; 23(5):599–619. <https://doi.org/10.1038/cr.2013.44> PMID: [23528706](https://pubmed.ncbi.nlm.nih.gov/23528706/)